Abstract for International Conference on Advances in Product Metallurgy of Long and Forged Products
July 12-15 2015, Vail, CO

High Strain Rate Hot Deformation of Steels: Measurement and Simulation

S. A. Rummel, D. C. Van Aken and R. J. O'Malley
Department of Materials Science and Engineering
X. Wang and K. Chandrashekhara
Department of Mechanical and Aerospace Engineering
Missouri University of Science and Technology, Rolla, MO 65409

Keywords: Hot Rolling, High Strain Rate, Constitutive Material Model, Rolling Simulation, Split Hopkinson Pressure Bar, Johnson-Cook Model

ABSTRACT

Local strain rates that occur during hot rolling of steel can range from very small up to rates above 1000 sec^{-1} and multiple experimental methods are required to develop a material model to predict plastic flow (stress and strain) behavior over this range. A Johnson-Cook model has been developed for 15V38 steel using experimental flow stress results in a temperature range of 1000°C to 1300°C and in a strain rate range of 0.1 s^{-1} to 30 s^{-1}. In addition, a split Hopkinson pressure bar was modified to measure the stress and strain behavior in a temperature range of 900°C to 1100°C and at strain rates near 1000 s^{-1}. The inclusion of split Hopkinson pressure bar data did not significantly affect the fit of the Johnson-Cook model coefficients at low strain rates; however, it improved the materials model for the intermediate and high strain rate ranges. Examples of finite element analysis (FEA) are shown to illustrate the hot rolling process simulation sensitivity to the applied material model.

INTRODUCTION

Importance of Hot Rolling Simulation

Hot rolling is the most common steel manufacturing process, which is used for over 85% of manufactured steel products.[1] Process development for hot rolling has often been experimental in nature, expensive with respect to industrial trials, and time intensive. Computational modeling of the hot rolling process offers a cost effective tool for designing roll profiles, determining working temperature ranges, and selecting rolling speeds to optimize the hot rolling process, in order to potentially improve product quality. A large portion of the investigations to date have examined the rolling of flat product, which can be reduced to a two dimensional simulation, and thus reduce the computation time by taking advantage of symmetry of the rolled product.[2] Improvements in computational software have led to powerful 3-D finite element analysis (FEA) with reduced mesh sizes to increase resolution and now offers the ability to model more complicated hot rolling processes. However, these complex rolled shapes require a more precise material model, since the flow of the material is more complex and may produce local plasticity with non-uniform strain rates.

Many commercial codes such as CORMILL, SIMURO, FORGE, CRC, and specialized modules within ABAQUS offer compositionally based material models, such as Shida's or Misaka's model, but these models are often restricted to plain carbon steel.[3,4] Compositionally based models have the benefit of being extremely easy to use, offering approximate stress-strain curves over a range of strain rates and temperatures.[5] Models like Shida's are not as accurate as a tailored constitutional model like the Johnson-Cook (JC) for specific steel compositions.

Even material models for plain carbon steels benefit from experimental verification and parameter adjustment, and the model can be constructed for the temperature, strain, and strain rate range of interest for the exact processing parameters. The main barriers to creating a custom material model are creating medium and high strain rate test conditions and the expense of the apparatus or testing service needed to generate elevated temperature results. A graphical representation of strain rates reported during the rolling process is shown in Figure 1. Typical ranges of observed strain rates for steel manufacturing are shaded in gray and the specific processes being studied for roughing and finishing are bracketed below the plot. It should be noted that the average strain rate range is distinct from the local strain rate that might be measured during the rolling of a complex shape.

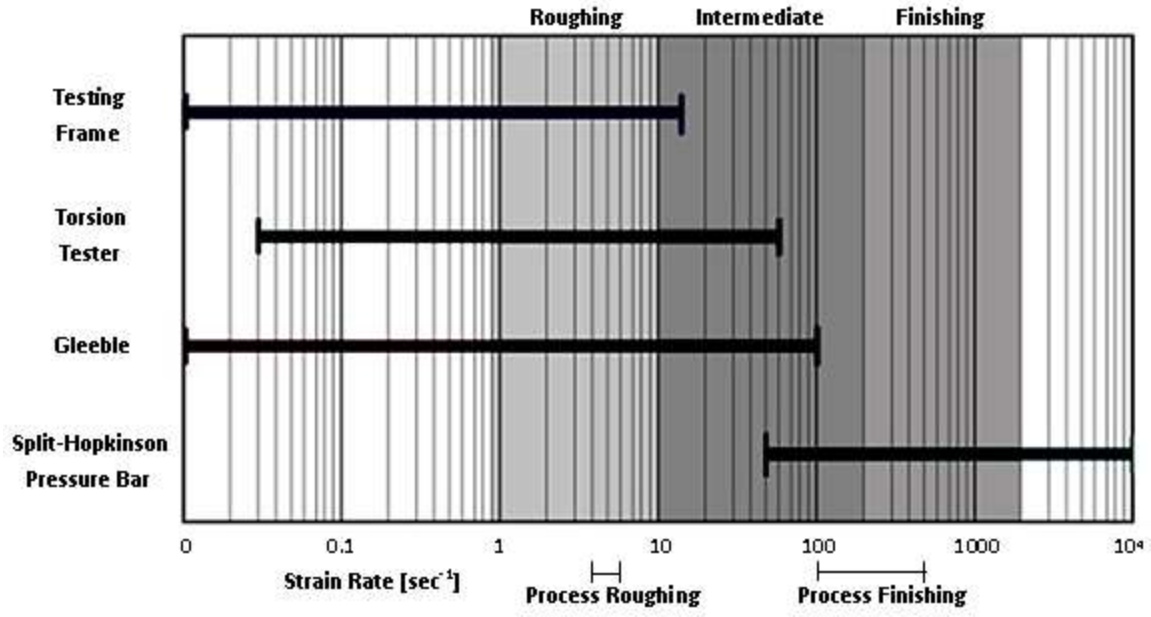

Figure 1. Graphical representation of industrial average and process specific strain rates for hot rolling, along with the range of strain rates covered by various experimental methods.

Gleeble thermo-mechanical simulators are widely used for strain rates below 50 s^{-1}, although rates up to 100 s^{-1} are claimed by the manufacturer. Torsion testing and standard mechanical test frames are also used to measure plastic flow behavior, but generally at strain rates less than 50 s^{-1}.[6,7] Higher strain rates, from 200 sec^{-1} to 5000 sec^{-1}, are substantially more difficult and fewer methods of generating this high strain rate data are available. Taylor testing and split Hopkinson pressure bar (SHPB) in compression are the most common ways of testing high strain rates at room temperature. High strain rate data can be used to develop models critical to simulate ballistics, and other high strain rate situations.[8] Lennon and Ramesh have successfully modified a split Hopkinson pressure bar to perform elevated temperature tests on Vanadium up to 1100°C and at strain rates as high as 4 x 10^3 s^{-1}.[9]

Material Models

An accurate material model for complex hot rolling operations is necessary in order to generate realistic finite element analysis (FEA) results. The ideal viscoplastic model would predict the flow stress using the deformation temperature, strain, and strain rate as well as take into account material history, i.e., previous strain hardening, and dynamic or static recovery or recrystallization. Commonly used models for modeling steel include Shida's,[4] Misaka's,[5] Johnson-Cook,[10,11] and Zerilli-Armstrong models.[10-12] A mathematical description containing all of the factors contributing to the flow stress of a material would be extremely complicated and possibly unnecessary, as some of these effects have a relatively small contribution under specific conditions. Assumptions can be made to reduce the number of contributing factors and simplify the resulting equation. In this study, two types of models were used. The first is Shida's Model, and the second is Johnson -Cook.

Shida's model predicts the flow stress (σ) of plain carbon steels at a particular strain (ε), strain rate ($\dot{\varepsilon}$), temperature (T), and carbon content (C).[5] This model accounts for the α↔γ phase transformation, covers carbon content in plain carbon steels from 0.07-1.2%, temperatures from 700-1200°C, strains up to 0.7, and strain rates up to 100 sec^{-1}:

$$\bar{\sigma} = \sigma_d(\bar{C}, T) f_w(\bar{\varepsilon}) f_r(\dot{\bar{\varepsilon}}) \quad (1)$$

where: $\sigma_d(\bar{C}, T)$ is the deformation resistance function and acts as a baseline flow stress for a specific carbon content at a specified temperature. The other two terms $f_w(\bar{\varepsilon})$ and $f_r(\dot{\bar{\varepsilon}})$, are the work hardening and strain rate hardening functions, respectively. Shida's model is similar to the Johnson-Cook model in that the final predicted flow stress is the result of the product of the three contributing functions, i.e. temperature, strain, and strain rate. Application of Shida's model does not require additional experimental data; however, because of the specialization to plain carbon steel it does not predict the flow properties of low alloy steels very well.

The *Johnson-Cook model* is built from a set of experimental data that is specific to a steel chemistry; however, there are no compositional inputs regarding the steel chemistry. Some commercial FEM programs include Johnson-Cook parameters for

some engineering materials.[3] This model is one of the most widely used material models in FEA largely due to the ease of incorporation into the computational programs.[10] In the Johnson-Cook model, the von Mises flow stress (σ) is represented by function of strain (ε), a dimensionless strain rate ($\dot{\epsilon}^* = \dot{\epsilon}/\dot{\epsilon}_0$), and homological temperature $T^* = \frac{T-T_r}{T_m-T_r}$:

$$\sigma = (A + B\epsilon^n)(1 + Cln\dot{\epsilon}^*)(1 - T^{*m}) \quad (2)$$

where: T is the temperature of interest, T_r, is a reference temperature, usually the lowest temperature that the model is used, and T_m is the melting temperature, A, B, n, C, and m are empirical coefficients used to fit the experimental test data. Softening effects are not taken into account, as the mathematical form of the model will not allow a decrease in flow stress. The Johnson-Cook model creates a direct relation between the strain hardening rate and the strain rate, but limits the accuracy when modeling materials that do not show an increase in strain hardening rate with increasing strain rate. However, the parameters can be selected to minimize this effect.

In this study, a combination of traditional low and medium strain rate tests were performed using a Gleeble themo-mechanical simulator and high strain rate tests using a modified split Hopkinson pressure bar test to build a comprehensive material model using a Johnson-Cook model. Of particular interest was to quantify the difference between using only the low and medium strain rates with a model that incorporated the high strain rate data obtained from the split Hopkinson pressure bar tests. The compositionally based Shida's model was also compared to the final Johnson Cook model.

EXPERIMENTAL PROCEDURE

Materials testing and modeling was performed for a special bar quality (SBQ) 15V38 steel with composition shown in Table I. The resulting model was used in modeling the two stand hot rolling of a round bar, which was also presented in this conference.[13]

Table I. Chemical composition of Vanadium micro-alloyed 15V38

	Fe	C	Mn	Si	Cr	V	Al	N	O
wt. %	Bal.	0.38	1.3	0.57	0.13	0.08	0.018	0.013	15 ppm

In Wang et al., a continuously cast round billet is hot charged into a walking beam furnace before entering the rolling mill. The hot rolling process consists of 12 stands that are paired into six sets, each with a horizontal roll stand and a vertical roll stand. Reduction by the first two roll stands deforms the cast circular cross section into an elliptical cross section and then deforms the elliptical cross section back into a near circular cross section. The hot rolling temperatures at these first two stands are approximately 1000-1250°C. The materials model used experimental data generated in the same temperature range using both a DSI Gleeble 3500 thermo-mechanical simulator with strain rates between 0.01 s^{-1} and 30 s^{-1} and a modified split Hopkinson pressure bar for high temperature flow stress measurement. Both experimental procedures are based on axisymmetric cylindrical compression testing.[14] Specimens for testing were machined from a 10" diameter as-cast 15V38 round billet, with the cylinder axis parallel to the casting direction.

Cylindrical Gleeble specimens were 10mm in diameter with a height of 15mm, with a tolerance of ±0.2 mm. Standard Gleeble tungsten platens were used for compression testing. Tantalum foil and nickel anti-seize paste between specimen and platens were used for lubrication to reduce barreling. The entire test fixture was located inside a vacuum chamber and tests were conducted under partial vacuum using a low helium flow rate. The maximum strain rate used was dictated by the testing fixture robustness and was less than 30 sec^{-1}. Testing included a baseline quasi-static test rate of 0.01 s^{-1}. Additional tests were conducted at 1, 5, 15 up to 30 s^{-1}. The testing temperature profile includes an austenitizing hold at 1300°C for 3 minutes, 260°C/min cooling to test temperatures of 1300°C, 1200°C, 1100°C, and 1000°C. The specimen was equilibrated using a 1 minute hold at the test temperature prior to compression testing. The initial austenitizing temperature of 1300°C mimicked the industrial as-cast condition and was above the VC and AlN precipitate stability temperatures.

The split Hopkinson pressure bar used for the high strain rate testing is shown in Figure 2a. The pressure bar consists of two 48" long and 1/2" diameter maraging 300 steel bars suspended in journal bearings, which provide free movement along the cylindrical axis. These bars, called the incident and anvil bars, are instrumented with strain gauges connected to a digital oscilloscope with a sampling rate of 5 MHz as shown in Figure 2b. The test specimen is placed in between the bars and a projectile is fired at the incident bar using a gas gun. The striker transfers a strain wave to the incident bar, which travels to the specimen bar interface, where, based on the modulus of the test material, a portion of the wave energy is transmitted and the remainder reflected. The transmitted portion of the wave continues into the anvil bar. A stress-strain curve can be calculated using the measured strain wave transmitted and reflected, the speed of sound in the bars, the modulus of the bars, and the area and length of the specimen. The pressure for the gas gun can vary from 25 psi to 90 psi, achieving a velocity range of 21 to 35 m/s. An induction coil has been added as a heating source and the test specimen is suspended in the

induction coil using a small sacrificial piece of compressed silica fiber board. Stepper motors with a rack and pinion configuration were used to mechanically move the pressure bars into contact with the heated sample just prior to firing the gas gun. The induction coil and specimen are surrounded by a plexiglass environmental chamber. An Argon gas flow into the environmental chamber is used to protect the sample from oxidation. A high resolution infrared pyrometer was focused onto the test specimen and the temperature was controlled directly by the test operator using the induction generator power.

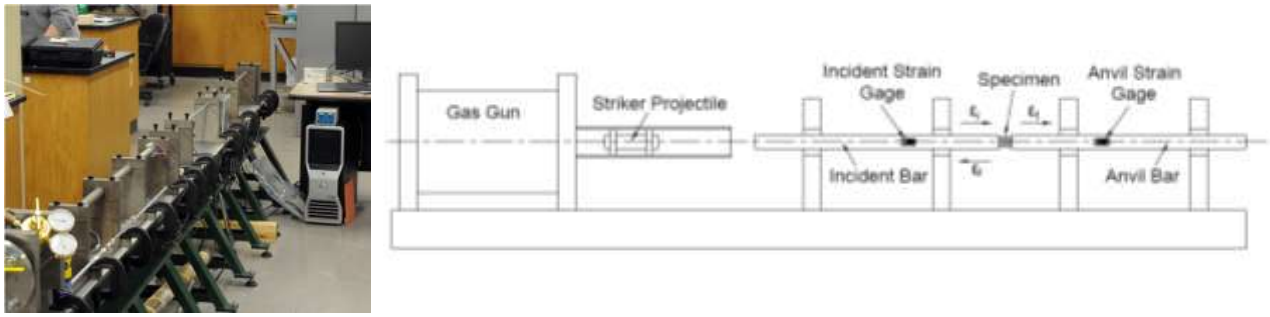

(a) (b)

Figure 2. Picture (a) and schematic (b) of Split Hopkinson Pressure Bar test apparatus modified for high temperature test.

A strain rate of approximately 1000 sec^{-1} was targeted; however, the strain rate is also a function of specimen length and the temperature dependent modulus. A specimen heating cycle consisted of a ramp to the test temperature, which generally took approximately 60 sec, and a 10 sec hold prior to moving the pressure bars into position and firing the gas gun. Test temperatures were reduced to 900°C, 1000°C, and 1100°C due to the expected adiabatic heating often incurred during high strain rate testing. Typical test data and its reproducibility are shown in Figure 3. The drop off in flow stress near the end of the stress-strain curve is an artifact of the testing, and results from a decreasing strain rate produced by the unloading time of the bar.

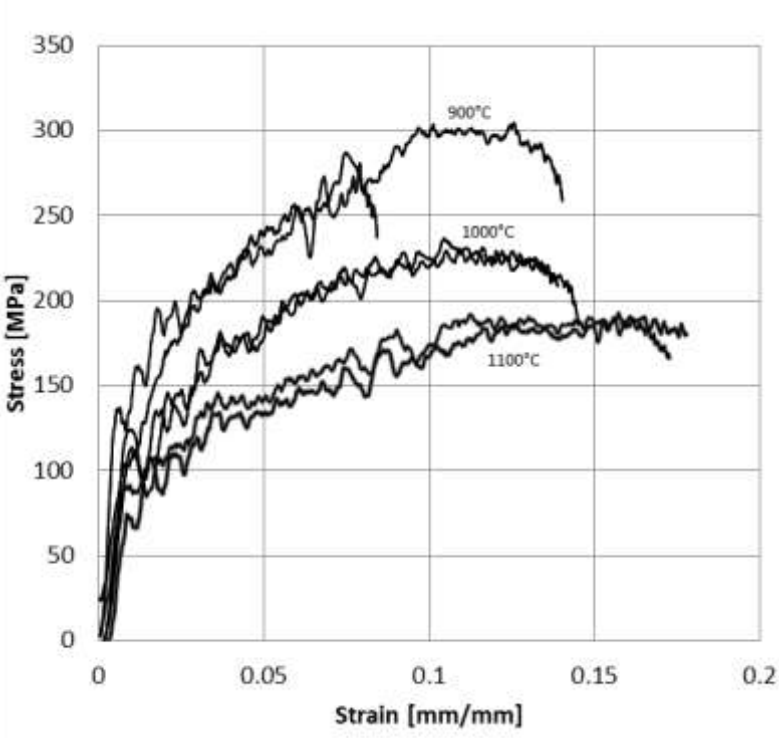

Figure 3. Example of repeated SHPB tests at various temperatures and a strain rate of ≈1000 sec^{-1}.

A non-linear regression analysis using excel solver was used to fit the Johnson-Cook model to the experimental data. The melting point of the steel was estimated to be 1520°C and this temperature was used as the T_m value. The lowest experimental point of interest was 850°C and this temperature was used for the lower bound T_r reference temperature. The

other values were set as variables that Excel solver could adjust to minimize the error, which was the average of the square of the differences between the model and data. The error was calculated for each curve and averaged to create overall error.

RESULTS

Figure 4 shows an example of tests at 1100°C with a wide variety of strain rates using both Gleeble and split Hopkinson pressure bar test data. It is clearly illustrated that flow stress increases with increasing strain rate as would be expected for austenitic iron. At the slowest strain rate of 0.01 s^{-1} the steel exhibits softening for strains greater than 0.18, which may indicate recrystallization. The flow stress remained constant after a strain of 0.3 to 0.4 for strain rates between 1 – 15 s^{-1} while significant hardening was observed at 1000 sec^{-1} strain rate.

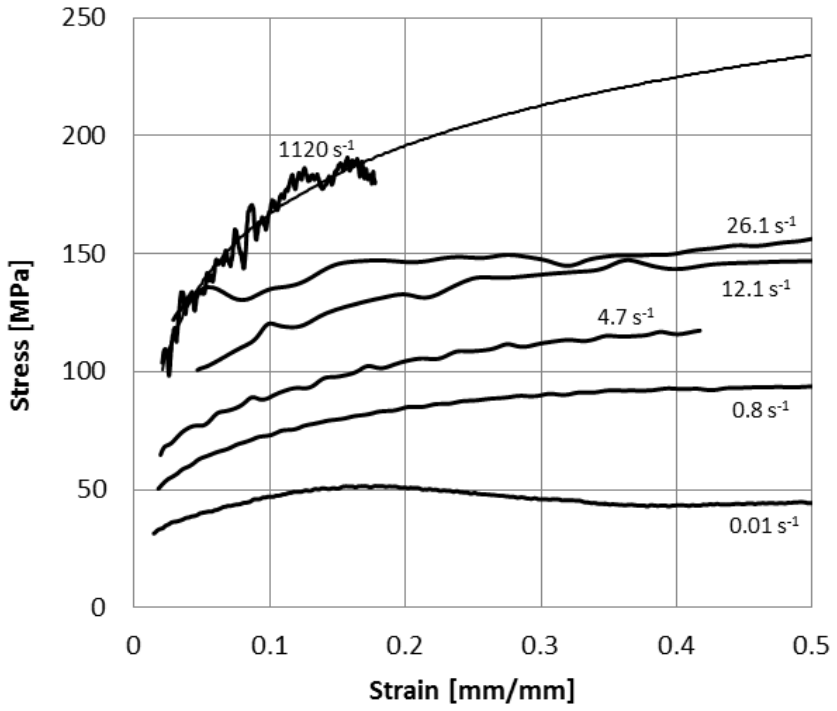

Figure 4. Example of experimental test results at 1100°C and the complete range of strain rates. Including a trendline extending the 1120 sec^{-1} strain rate to higher strains

Two nonlinear regression analyses were performed, the first one was based on only the Gleeble data and the second one included all low, medium, and high strain rate data from Gleeble and split Hopkinson pressure bar tests (see Table II).

Table II. Calculated JC parameters for Gleeble tests and for joint Gleeble and SHPB tests

Constants	Model 2	Model 3
A	75.0	75.0
B	127	166
C	0.124	0.119
m	1.07	0.86
n	0.248	0.266
Tm	1520	1520
Tref	849	849
e'ref	1.00	1.00

DISCUSSION

In this study three sets of stress-strain models were built and compared:

-Model 1 – Shida's equation prediction for 15V38

-Model 2 - JC approximation of Gleeble experimental tests at 0.01-30 sec^{-1} strain rates

-Model 3 - JC approximation of both Gleeble and SHPB experimental test at 0.01-1000 sec^{-1} strain rates

Comparison of experimental data with predicted from Model 1 (Shida's approximation), Model 2 (JC at low/medium strain rates) and Model 3 (JC at all studied strain rates) is given in Figure 5 for 1000°C at different strain rates. Figure 6 shows flow stresses at 0.2 strain for the three models in comparison to experimental results. In both figures it can be seen that Shida's model consistently underestimates the flow stress.

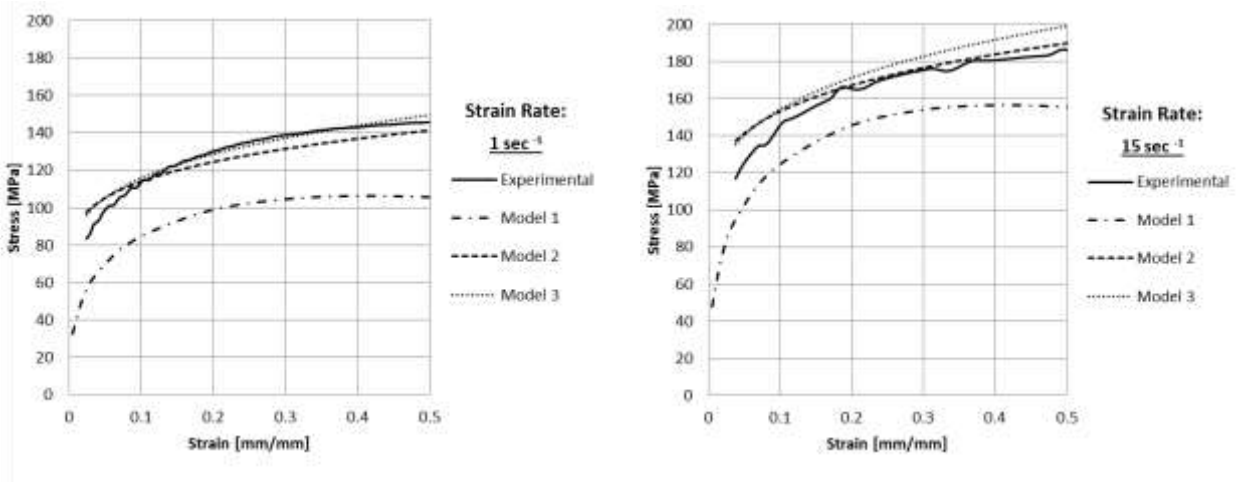

(a) **(b)**

Figure 5. Experimental and predicted from Model 1 (Shida's) and Model 3 (JC model based on approximated Gleeble and SHPB tests) at 1000°C: (a) 1 sec-1 and (b) 15 sec-1 strain rates.

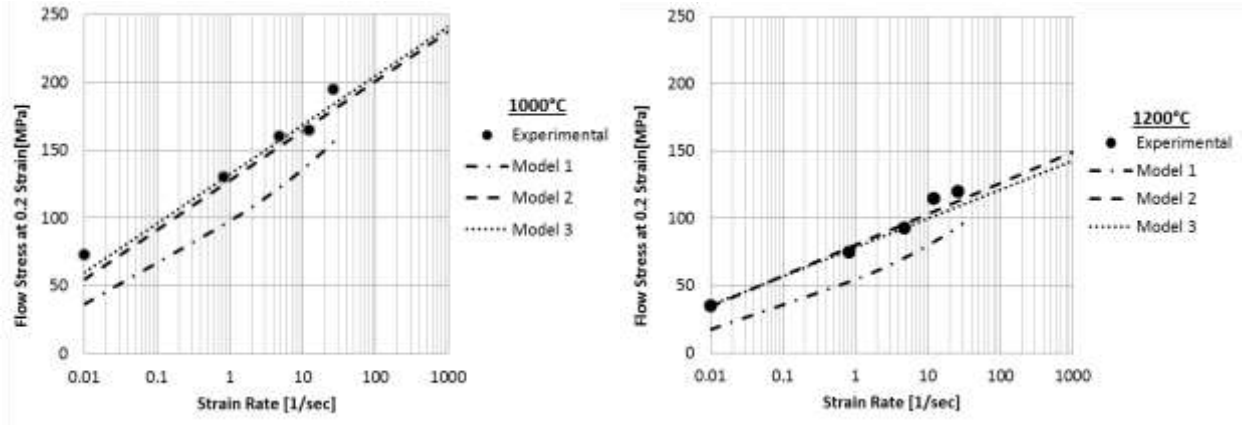

(a) **(b)**

Figure 6. Comparison of experimentally measured flow stress with predicted from Model 1 (Shida's), Model 2 (JC model based on Gleeble Tests), and Model 3 (JC model based on approximated Gleeble and SHPB tests)

The importance of high strain test data can be seen in comparing Model 2 (based on Gleeble data alone) as shown in Figure 7a and Model 3 (Gleeble and SHPB data) as shown Figure 7b with the actual experimental results obtained with SHPB test apparatus. The incorporation of the SHPB experimental data along with the Gleeble data in Model 3 statistically improved predictions. The coefficient of determination, or R^2, compares each curve to the average of the experimental model and is used to compare the fit of models. The R^2 for (7a) is 0.56 and for (7b) is 0.80.

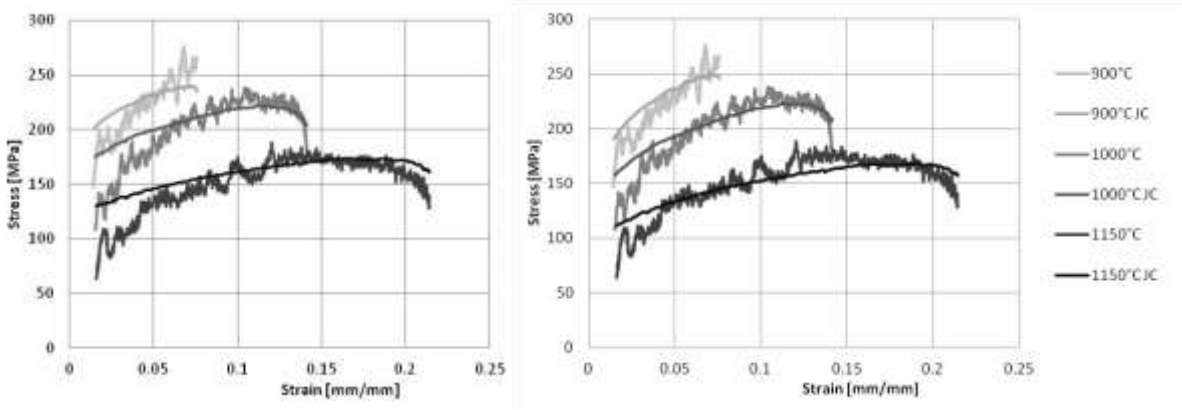

(a) (b)

Figure 2 . Comparison of experimental stress-strain curves obtained at high strain rate (apr 1000 sec^{-1}) with predicted: (a) from Model 2 (JC based on Gleeble test) and (b) from Model 3 (JC based on both Gleeble and SHB)

The difference in the fit of each model to each set of data is shown in Table III, where it can be seen that inclusion of the SHPB results has not significantly affected the fit of the low strain rate data and has improved the fit of the high strain rate data.

Table III. The average R^2 statistical comparisons of predicted stress from Model 1, (Shida's), Model 2 (JC based on Gleeble) and model 3 (JC based on Gleeble and SHPB) for the Gleeble and SHPB data over all temperatures.

R^2 Values		
Model	**Gleeble**	**SHPB**
1	0.51	-
2	0.92	0.56
3	0.91	0.8

The inclusion of SHPB data into JC model 3 changes some of parameters in model 2 built using only the Gleeble tests. The biggest differences were an increase in the strengthening parameter, a reduction of the effects of temperature softening, and an increase in strain hardening rate. All three of these effects can be partially attributed to the fact that the low strain rate testing has some softening effects, which are difficult to separate out from the pure flow stress data. This leads to the under-calculation of base strengths, as the material is softening before reaching the maximum stress. This under-calculation is compensated by a higher temperature dependent effect.

An example of the effect of each material model on FEA hot rolling process is given in Figure 8. It could be seen that changing material model at the same hot rolling parameters had significant effects on the predicted stress.

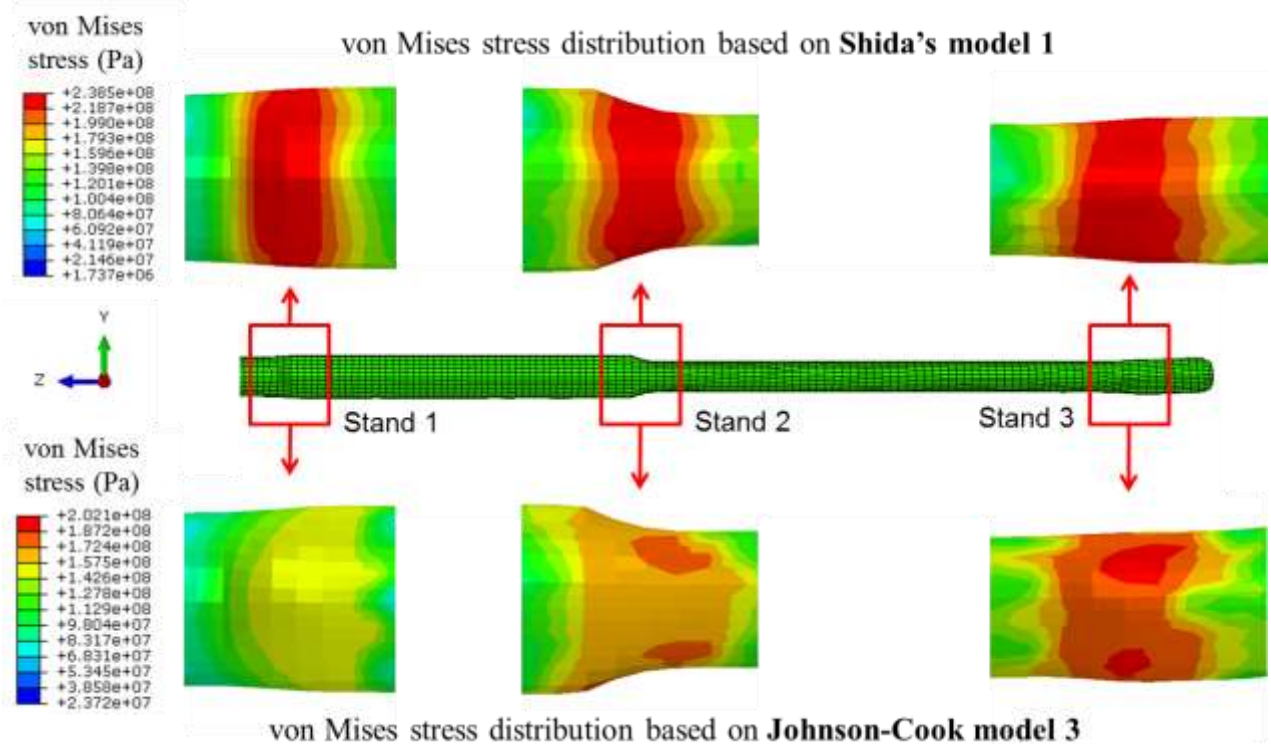

Figure 8. Overhead view of FEM simulated hot rolling process applying Model 1 (Schida) and Model 3 (JC based on Gleeble and SHPB tests).

CONCLUSIONS

As expected, Shida's model could not predict the flow stress behavior of a low alloy steel such as 15V38. A Johnson-Cook model was developed using only Gleeble testing and resulted in a better fit to the experimental data. Inclusion of high temperature split Hopkinson pressure bar data further improved the model by better predicting the flow stress at low strains. The inclusion of the SHPB data improved the R^2 value for the high strain rate data from 0.56 to 0.80. The high temperature SHPB produced repeatable high strain rate data at elevated temperatures. The successful inclusion of the experimental data into a JC model opens the possibility for better prediction of material flow over a greater range of strain rates and temperatures.

ACKNOWLEDGMENTS

This work was supported by the Peaslee Steel Manufacturing Research Center at Missouri University of Science and Technology. The authors would like to thank Dr. Simon Lekakh for his advice and guidance, Mario Buchely Camacho for lending his SHPB expertise, Geary W. Ridenour, Mike Kolljeski and Ross Wilkinson from Gerdau-Fort Smith for their practical input. Finally, Todd Link from US Steel Corporation and Rafael Pizarro Sanz from Gerdau Aceros Especiales Europa for Gleeble testing.

REFERENCES

1. AISI Technology Roadmap Research Program for the Steel Industry 2010

2. S.X. Zhou, An Integrated Model for Hot Rolling of Steel Strips. *Journal of Material Processing Technology*, Vol. 134, 2003, pp.338-351

3. S. Biswas, "Simulation of Thermo-mechanical Deformation in High Speed Rolling of Long Steel Products." Master's Thesis, Worcester Polytechnic Institute 2003

4. S. Byon, D. Na, and Y. Lee, "Flow stress equation in range of intermediate strain rates and high temperatures to predict roll force in four-pass continuous rod rolling." *Trans. Nonferrous Met. Soc. China*, Vol. 23, 2013, pp.742-748

5. Y. Leea, B. Kimb, K. Parkc, S. Seob and O Minc "A Study for the Constitutive Equation of Carbon Steel Subjected to Large Strains, High Temperatures and High Strain Rates." *Journal of Materials Processing Technology*, Vol. 130-131, 2002, pp. 181-188

6. R. Kawalla, W. Muller, and W. Jungnickel, "Physical Simulation at Hot Deformation." *Material Science Forum*, Vol. 638-642, 2010, pp.2591-2597

7. J.J. Jonas, X. Quelennec, and L. Jiang, "Modeling the Flow Curve of Hot Deformed Austenite" *Materials Science Forum*, Vol. 715-716, 2012, pp.81-88

8. M. Huang, "Ballistic Resistance of Multi-layered Steel Shields." MS Thesis, MIT 2007

9. A.M. Lennon and K.T. Ramesh, "A Technique for Measuring the Dynamic Behavior of Materials at High Temperatures." *International Journal of Plasticity*, Vol. 14, No. 12, 1998, pp. 1279-1292

10. R. Liang and A.S. Khan, "A Critical Review of Experimental Results and Constitutive Models for BCC and FCC Metals Over a Wide Range of Strain Rates and Temperatures." *International Journal of Plasticity*, Vol. 15, 1999, pp. 963-980

11. N. Fang, "A New Quantitative Sensitivity Analysis of the Flow Stress of 18 Engineering Materials in Machining." *Journal or Engineering Material Technology*, Vol. 127, No. 2, 2005, pp.192-196

12. F. H. Abed and G. Z. Voyiadjis, "A Consistent Modified Zerilli-Armstrong Flow Stress Model for BCC and FCC Metals for Elevated Temperatures." *Acta Mechanica*, Vol. 175, 2005, pp. 1-18.

13. X. Wang, K. Chandrashekhara, S. A. Rummel, S. Lekakh, D. C. Van Aken and R. J. O'Malley, "Modeling and Simulation of Hot Rolling using Nonlinear Material Models," AIST Long and Forged Products Symposium, Vale, Colorado, July 2015

14. B. Kowalski, C.M. Sellars and M. Pietrzyk: "Identification of Rheological Parameters on the basis of Plane Strain Compression Tests on Specimens of Various Initial Dimensions" *Computational Material Science* Vol. 35 2006, pp. 92-97